



A compact olfactometer for IMS measurements and testing human perception

Citation

Nieminen, V., Karjalainen, M., Salminen, K., Rantala, J., Kontunen, A., Isokoski, P., ... Lekkala, J. (2018). A compact olfactometer for IMS measurements and testing human perception. *International Journal for Ion Mobility Spectrometry*, 21(3), 71-80. <https://doi.org/10.1007/s12127-018-0235-1>

Year

2018

Version

Peer reviewed version (post-print)

Link to publication

[TUTCRIS Portal \(http://www.tut.fi/tutcris\)](http://www.tut.fi/tutcris)

Published in

International Journal for Ion Mobility Spectrometry

DOI

[10.1007/s12127-018-0235-1](https://doi.org/10.1007/s12127-018-0235-1)

Take down policy

If you believe that this document breaches copyright, please contact cris.tau@tuni.fi, and we will remove access to the work immediately and investigate your claim.

A COMPACT OLFACTOMETER FOR IMS MEASUREMENTS AND TESTING HUMAN PERCEPTION

ABSTRACT

Production of easily controllable and measurable odor stimuli is needed when studying human olfaction, olfaction-related physiology and psychological reactions to odors. Controlled odor producing instruments are called olfactometers. For testing and calibrating new olfactometers or sensor arrays, a reliable input signal has to be produced to verify their accurate functionality. A common input signal in various olfactometers has been the use of volatile organic compounds (VOCs) in gaseous form.

We present a compact olfactometer able to produce controlled continuous odor stimuli from three individual channels. For measuring the output gas flow, we used a ChemPro 100i (EnviroNics, Finland) device that is based on aspiration ion mobility spectrometry (aIMS). IMS is a robust and sensitive method for measuring VOCs and is used especially in detecting toxic industrial chemicals and chemical warfare agents, but the technology is also suitable for other olfactory-related applications.

The olfactometer was used to produce synthetic jasmine scent using three main odor components from jasmine oil and all the components were diluted using propylene glycol. The dilutions were supplied to the system using programmable syringe pumps, which guided the dilutions to individual evaporation units. We conducted experiments to verify the functionality of our olfactometer. Analysis of the ChemPro100i data showed that olfactometer can use different odor components to produce continuous, stable output flows with controlled concentrations.

1. Introduction

Odors have a significant role in human cognition, emotions, and behavior. Odors are known to have a positive effect on memory and emotions, they can control appetite, and even help in identifying if food is edible (Chu and Downes, 2000; Bensafi *et al.*, 2003; Stevenson, 2010). The abnormalities in the sense of smell are present in several medical conditions including neurodegenerative diseases (Doty, Reyes and Gregor, 1987), other cognitive impairments (Hedner *et al.*, 2010), and severe obesity (Richardson *et al.*, 2004). Thus, there is a clear need for studying the functioning of the sense of smell in both societal and individual level. When developing olfaction instruments or studying human olfaction and physiological, behavioral, and psychological responses to odors, production of easily controllable and measurable odorous stimulus is imperative. This is the only way to gain detailed and generalizable information about olfaction that can be used, for instance, in learning applications or to find out if someone is in a risk of developing decreased cognitive functioning.

Therefore, creating a system, which is capable to objectively and reliably classify a wide range of odors is a key research question in the field of artificial olfaction. So far, the produced odor detectors are in most cases optimized to only sense specific molecules or compounds that are relevant to their specific applications. Thus, they do not provide the same potential sensitivity to the complex world of odorants as the mammalian olfactory systems. Over the latest decades, various kinds of unique odor sensors with different kind of sensing materials and detection principles have been developed, including sensors based on olfactory receptors extracted from or used in alive insects or animals (Utriainen, Kärpänoja and Paakkanen, 2003; Huotari, 2004; Nakamoto, Kakizaki and Suzuki, 2004; Glatz and Bailey-Hill, 2011; Brooks *et al.*, 2015). The more common sensor types used in artificial olfaction are semiconducting metal oxide sensors (MOS), catalytic field-effect sensors (MOSFET), conducting polymer sensors, electrochemical sensors, and optical sensors (James *et al.*, 2005; Wilson and Baietto, 2009).

Examples of previous work related to classifying odors include Tang *et al.* who presented a sensor array consisting of eight sensors, which is capable of identifying three different fruits (Tang *et al.*, 2010) and Omatu *et al.* who used data from 14 metal oxide semiconductor gas (MOG) sensors, each sensitive to different main detecting gas, to classify odors from different species of coffee and tea (Omatu, 2013). Artificial olfactory systems have been used at least for disease diagnostics (Friedrich, 2009; Wilson and Baietto, 2009; Gutiérrez and Horrillo, 2014), industry (Giordani *et al.*, 2007; Berna, 2010; Fang *et al.*, 2010), entertainment, military, and security (Kolakowski *et al.*, 2007) purposes. Applications such as determining shelf-life of food products (Schaller, Bosset and Escher, 1998; Benedetti *et al.*, 2005; Labreche *et al.*, 2005), detecting emissions from polluted rivers (Lamagna *et al.*, 2008), and detecting lung cancer from the breath (Phillips *et al.*, 2003) have also been presented.

Several scent delivering olfactometer instruments have been developed and described (Schmidt and Cain, 2010; Sommer *et al.*, 2012). Schmidt *et al.* have studied olfactometry and threshold measurements. They presented a system called vapor delivery device 8 (VDD8). VDD8 includes a syringe pump injection vapor stabilizing chamber, called vapor capacitor, optional two stage pre-dilution with nitrogen and odor stream, and eight constant flow rate dilutors (Schmidt and Cain, 2010). Sommer *et al.* presented a mobile olfactometer that was used with fluorescence magnetic resonance imaging (fMRI) to study the dependence of identifying smells and activation of different regions of the brain (Sommer *et al.*, 2012).

For olfactometers, calibration, validation, and feedback measurements from the odor concentration and for odor chemical composition, are highly recommended (Schmidt and Cain, 2010). Commonly used calibration or reference

methods include gas chromatography (GC), High-Pressure Liquid Chromatograph (HPLC), and Photo Ionization Detector (PID) (Lundström *et al.*, 2010). Ion mobility spectrometry (IMS) is a robust, simple, and sensitive method for measuring volatile compounds. We decided to apply an aspiration ion mobility spectrometer (aIMS) for the measurements instead of more complex methods, due to its simplicity, cost, and robustness. The aIMS-device is also intended for mobile use which enables use outside laboratory environment. Here we present the combined aIMS-olfactometer (aIMS-O) instrumentation, experiments and results. Our aim was to vary the concentration of different odor components using the aIMS-O instrument. The possibility to vary the concentrations of individual odor components is valuable as odor mixtures from the same odor components can be perceived completely differently with different concentrations. (Auffarth, 2013; Thomas-Danguin *et al.*, 2014)

2. METHODOLOGY AND MATERIALS

The aim of the presented instrumentation is to use low cost components in order to produce different odor components in a gas phase with different concentrations. The odor of interest in this paper is jasmine oil and synthetic versions of jasmine oil created using three of its main components. In order to be able to vary concentrations of the odor components, each component was evaporated in an individual evaporation unit. The schematic representation of the design can be seen in Figure 1.

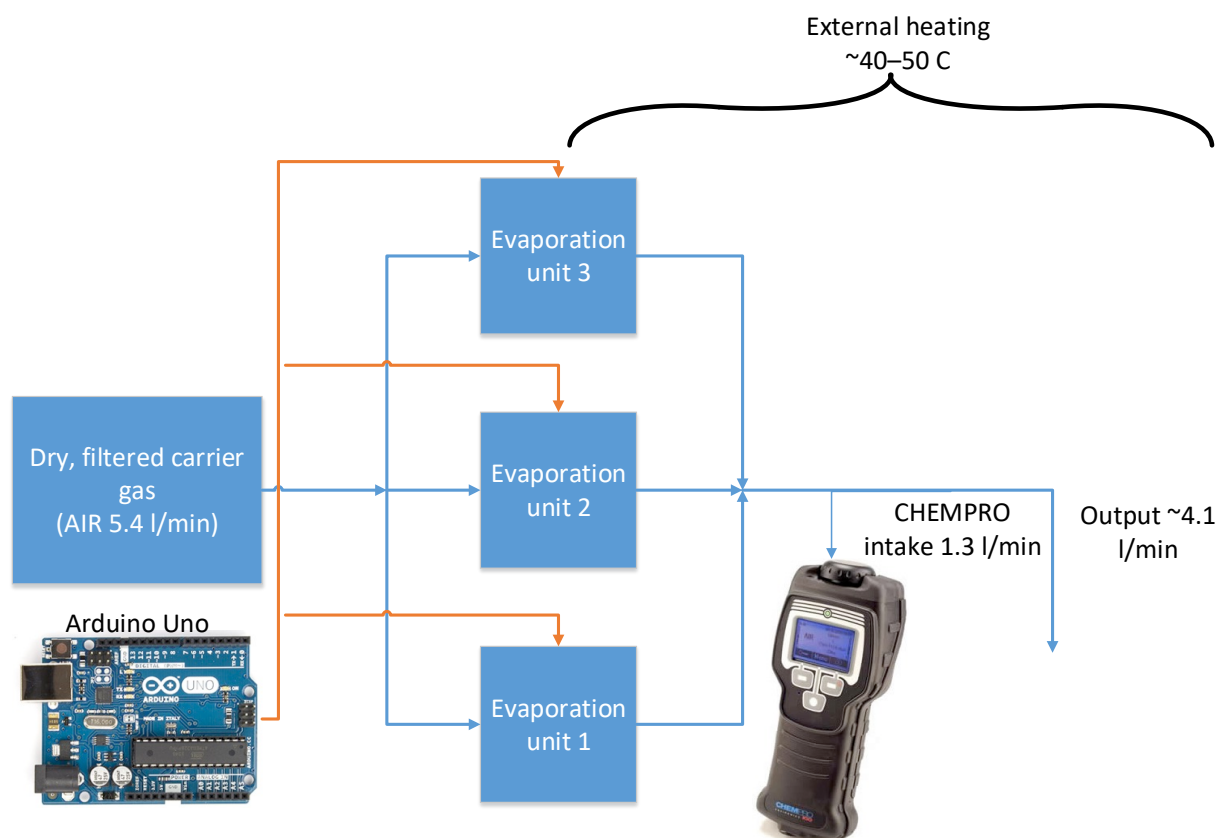


Figure 1. Block diagram of our aIMS-O instrument. Dry, filtered air is directed to three channels each having a flow of 1.8 l/min. Each channel has an evaporation unit whose power is controlled by Arduino microcontroller. The output of the instrument is monitored with ChemPro 100i chemical detector.

Each of the three evaporation units consist of standard 6 mm pneumatic components (polytetrafluoroethylene tubing and steel connectors with nitrile O-rings), a ceramic heater element, and a polyether ether ketone (PEEK) tube that connects the syringe tubing to the surface of the heater element. An illustration and a photograph of an evaporation block are presented in Figure 2. PEEK has a high glass transition temperature of 143 °C, which makes the placement of the tube on the heater surface possible. Higher temperatures are prohibited to ensure durability. For the heating elements used, the surface temperature of 140 °C corresponded to approximately 1.5 W of input power.

The olfactometer has designed for three different odor components since as according to several studies human nose seems to be able to distinguish three or four individual odor components from complex mixtures (Laing and Glemarec,

1992; Livermore and Laing, 1998; Guichard, 2017). In this paper, we demonstrate the use of the three channels for three main components found in jasmine oil. These components are benzyl acetate (BEA), 3-methyl-2-[(Z)-pent-2-enyl]cyclopent-2-en-1-one (also known as Cis-Jasmone, (CIS)) and 1H-Indole (IND). As IND is in powder form in standard room conditions, we diluted the components using propane-1,2-diol (also known as Propylene glycol, PG). Even though PG is a viscous, colorless and odorless liquid, using a diluent is not an ideal solution as it also produces signal in the IMS unit and the data processing and analysis becomes more complex. Using diluted solutions where the diluent is the main component was beneficial in terms of making the different solutions similar in properties, most importantly the vapor pressure. Similar properties between the components made it possible to use the same power control settings for each of the three components.

We used air as the carrier gas and it was dried and purified with activated carbon and 5Å molecular sieves (Alfa Aesar, Germany). The flow of the carrier gas was controlled by a Q-flow rotameter (Vögtlin Instruments, Switzerland) and each channel had a flow of 1.8 l/min. The flows were verified using a Gilian Gilibrator-2 NIOSH Primary Standard Air Flow Calibrator (Sensidyne, Schauenburg International GmbH, Germany).

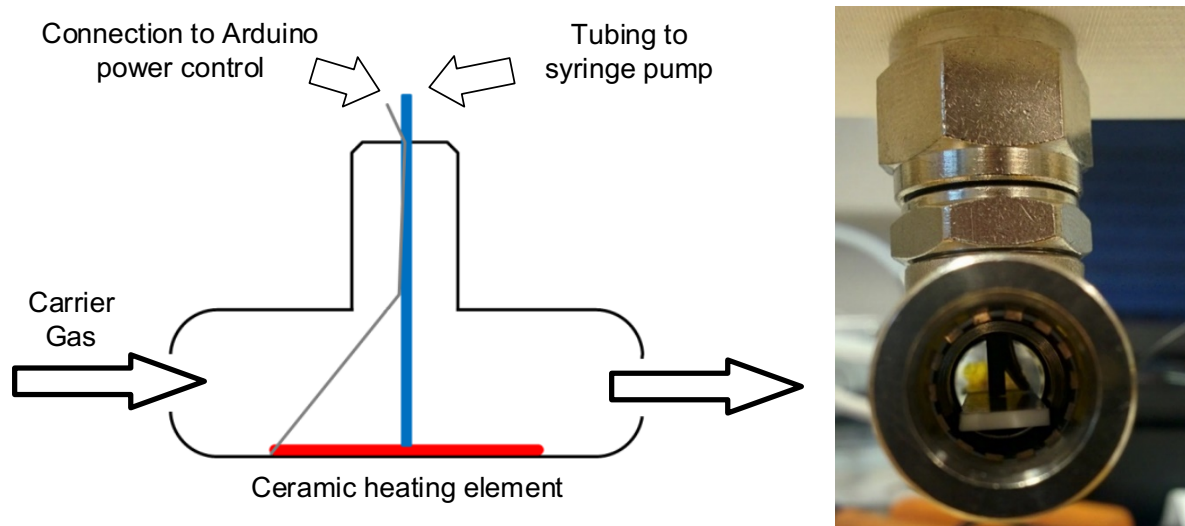


Figure 2. The structure of the evaporation unit. Odorous sample is injected from the syringe pump through the PEEK-tube to the surface of the heating element. Power of the heating element is changed according to the pumping speed.

The diluted odor components were injected to the evaporation units using syringe pumps, one for each odor component. The pumps used were Newera NE-500 (New Era Pump Systems, USA) programmable syringe pumps and were controlled with Matlab. The pumps were controlled by programming different operation phases to the pumps. Each operation phase is responsible for a certain task, e.g. pumping with a certain speed and for a certain time, stopping or waiting a certain time before moving to next phase. For our system, the most important requirement of the pumps was the ability to produce stable, constant pumping with a known flow rate. The motors controlling the syringe pumps are 400 step stepper motors, and they are the limiting factor when trying to produce odor concentrations with the lowest possible pumping speed as individual steps of the motors start to be distinguishable and the mass flow is not constant enough to produce stable gas concentrations.

We controlled the electric power of the heating elements using a MOSFET power circuit built on Arduino proto shield (Figure 3). Based on the gate voltage of each MOSFET, the voltage and the current over and through the heating element changes. Different heating powers were used with different pumping speeds to keep the evaporation capability

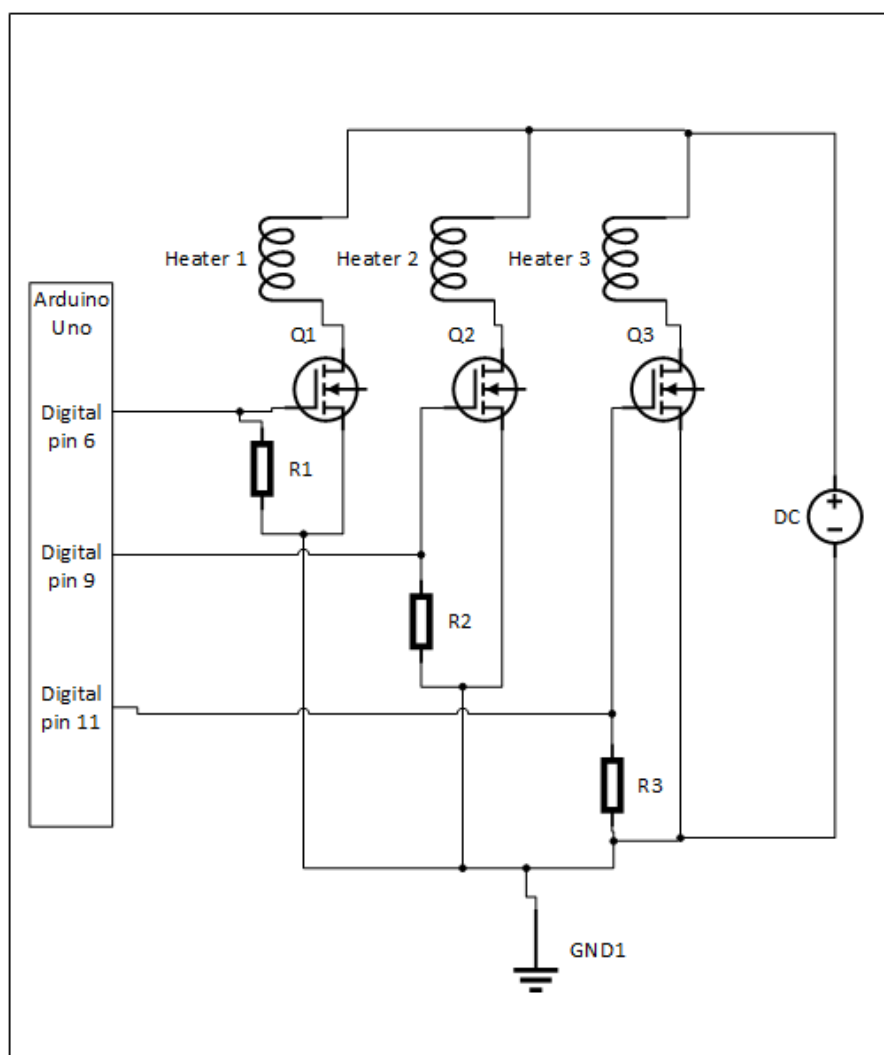


Figure 3. Schematic of the Arduino Proto Shield -circuit used to control the powers of the ceramic heating elements. The gate voltages of the MOSFETs (Q1, Q2, Q3) are controlled using analog voltage signals from three digital pins in Arduino Uno. According to the gate voltage, the heating power of the heaters change accordingly.

of the heater compatible with the volume being pumped. After initial experiments, a linear relationship between the heater power and the pumping speed needed to achieve stable evaporation was found. Based on the found relation between the heater power and the pumping speed, an automated power control was designed. A function was written to read corresponding pumping speed and gate voltage -pairs and set the voltages on corresponding Arduino pins.

The produced gas concentration and evaporation were considered stable, when after ten minutes from starting the pumps, 14 ion detecting ChemPro-channels had reached a steady-state value from clean air baseline readings to certain levels and after the pumps were stopped, the channels returned to baseline values within ten minutes. In addition to the 14 ion detecting plates, ChemPro 100i records data for a total of 59 parameters. These include external and internal temperatures, date, time, and other metadata. The data used in this paper for analysis, as well as for the Sammon map

projections described later, is from the 14 ion detecting channels. The usefulness of other parameters provided by ChemPro 100i in this context needs to be further evaluated.

To stabilize the temperature conditions, we installed an HTWAT Series silicone rubber heating tape (Omega Engineering, USA) to cover the part of the system after the evaporation blocks. By applying external heating, we achieved two main benefits; the possibility of condensation of the odor components in the system decreases and the time it takes for the system to be clean, meaning that the time all the residues from the pneumatic tubing and connectors are evaporated, is shorter. Secondly, the varying heater powers and external temperature changes (which were present in our laboratory environment) do not affect the temperature of the system as much as before applying external heating, which makes the overall system temperature and the observed ChemPro100i cell temperature more stable. The ChemPro100i has a built-in heater, which eventually stabilizes the temperature in the device between 32 and 37 degrees of Celsius in our laboratory conditions, depending on the external temperature. With the external heating tape, the cell temperature stabilizes to 34-36 °C faster and with less variation. Stable temperature is important to get reliable and consistent signals from the IMS-device as changes in temperature affect the signals particularly when detecting molecules that belong to the thermodynamic group with low proton affinity (PA). (Eiceman, Karpas and Hill, 2013)

The temperature of the system was observed using a FLIR One heat camera (FLIR Systems Inc., USA). Figure 4 shows that the temperature is homogeneous for the part of the olfactometer tubing covered with the rope heater. The only “hot spot” is the adapter connecting the three channels together, but this should be a minor problem as all the channels go through the adapter and thus, the situation for all the channels is the same. Furthermore, it is advantageous that the adapter, being also a possible source of residual odors having metallic parts, is heated slightly more for faster cleansing. In our experience, the metallic adapter did not affect the produced odor in a noticeable way.

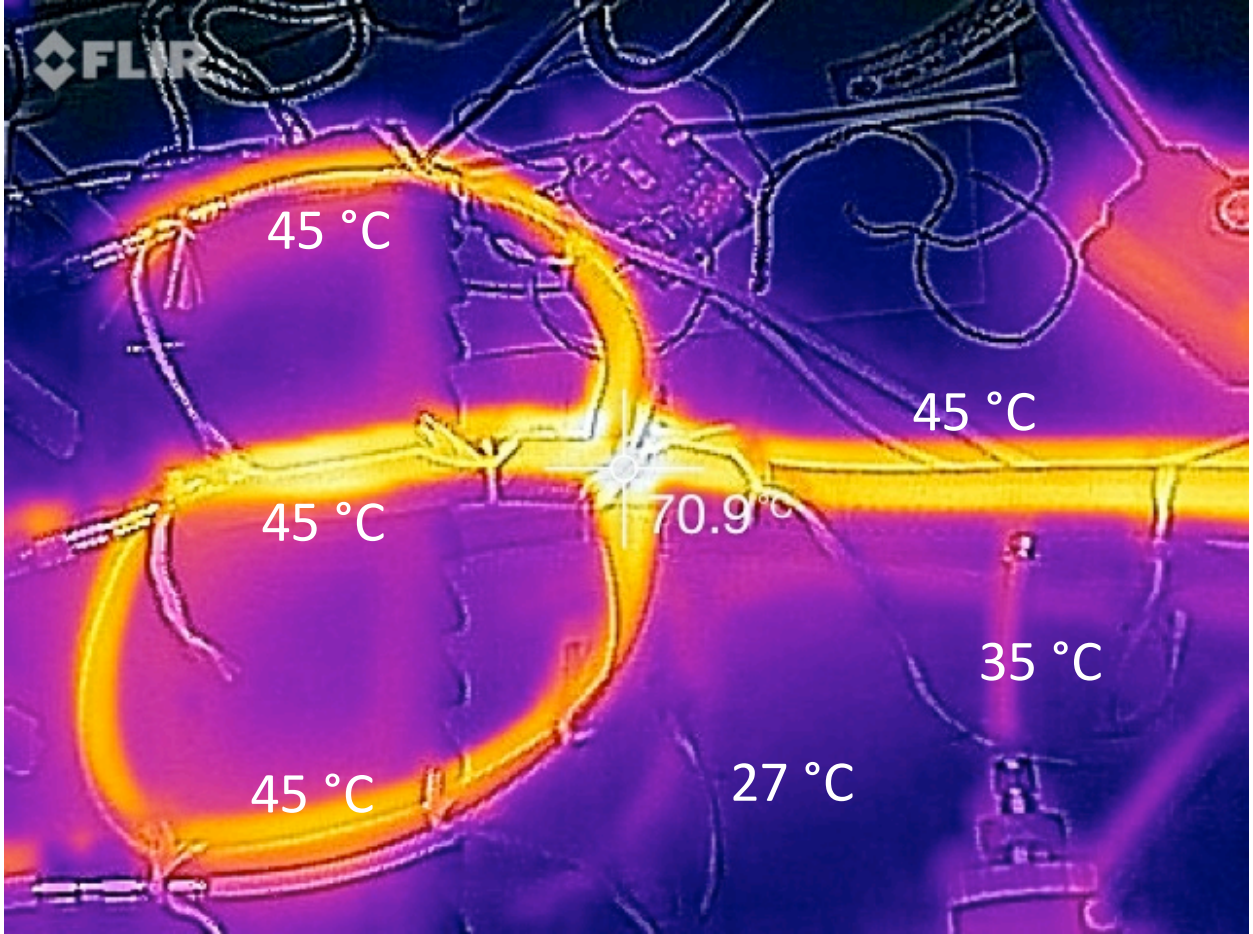


Figure 4. Thermal image of the part of sample handling system covered with HTWAT series heating tape.

The measurement data from ChemPro 100i is recorded using software provided by the same manufacturer, Environics. The rest of the system is controlled with MATLAB (The MathWorks Inc., U.S.A). The concentration of the odor component is determined by selecting a proper pumping speed. The relationship between gas mass concentration and pumping speed was calculated by first determining the volume of an odor component in the solution

$$V_o = \frac{mp \cdot \rho_{pg} \cdot V_{tot}}{(1-mp) \cdot \rho_o + mp \cdot \rho_{pg}}, \quad (1)$$

where mp is the mass percentage of the odorant in the solution, ρ_{pg} and ρ_o are the densities of the dilutant and odorant. V_{tot} is the total volume of the solution. As the values to control the syringe pumps are in the order of $\mu\text{l/hr}$, all the volumes used in calculations are given for one hour of operation.

With known properties for the carrier gas, the resulting mass concentration of the odorant in the output gas flow is calculated from

$$ppm_o = \left(\frac{\rho_o \cdot V_o}{\rho_a \cdot V_a + \rho_o \cdot V_o + \rho_{pg} \cdot V_{pg}} \right) 10^{-6} \quad (2)$$

where V_{pg} is the volume of the dilutant and ρ_a and V_a are the density and volume of the carrier gas.

When considering the concentration range in logarithmic scale, the range able to be achieved with our system by varying the pumping speeds is approximately one decade. Figure 6 demonstrates the estimated concentrations produced with the aIMS-O instrument. As each of our components is diluted with propylene glycol, the “location” of the decade on the ppm scale is determined by the concentration of the odorant in the solution. The selected pump rate determines the mass concentration of the odor component produced in the gas output according to Equation (2). For example, in the conducted measurements, the most used concentrations for BEA and CIS in the syringes was 15 % (w/w). This concentration locates the range in 10-100 ppm and the exact gas concentration within this range can be decided by selecting one of the identified pump rates in Fig. 5.

Additional dilution stage can be applied by using an ejector in the output of the system. Dilution with an ejector affects all the components when applied in the output where all the odor components are present. This means that with ejector

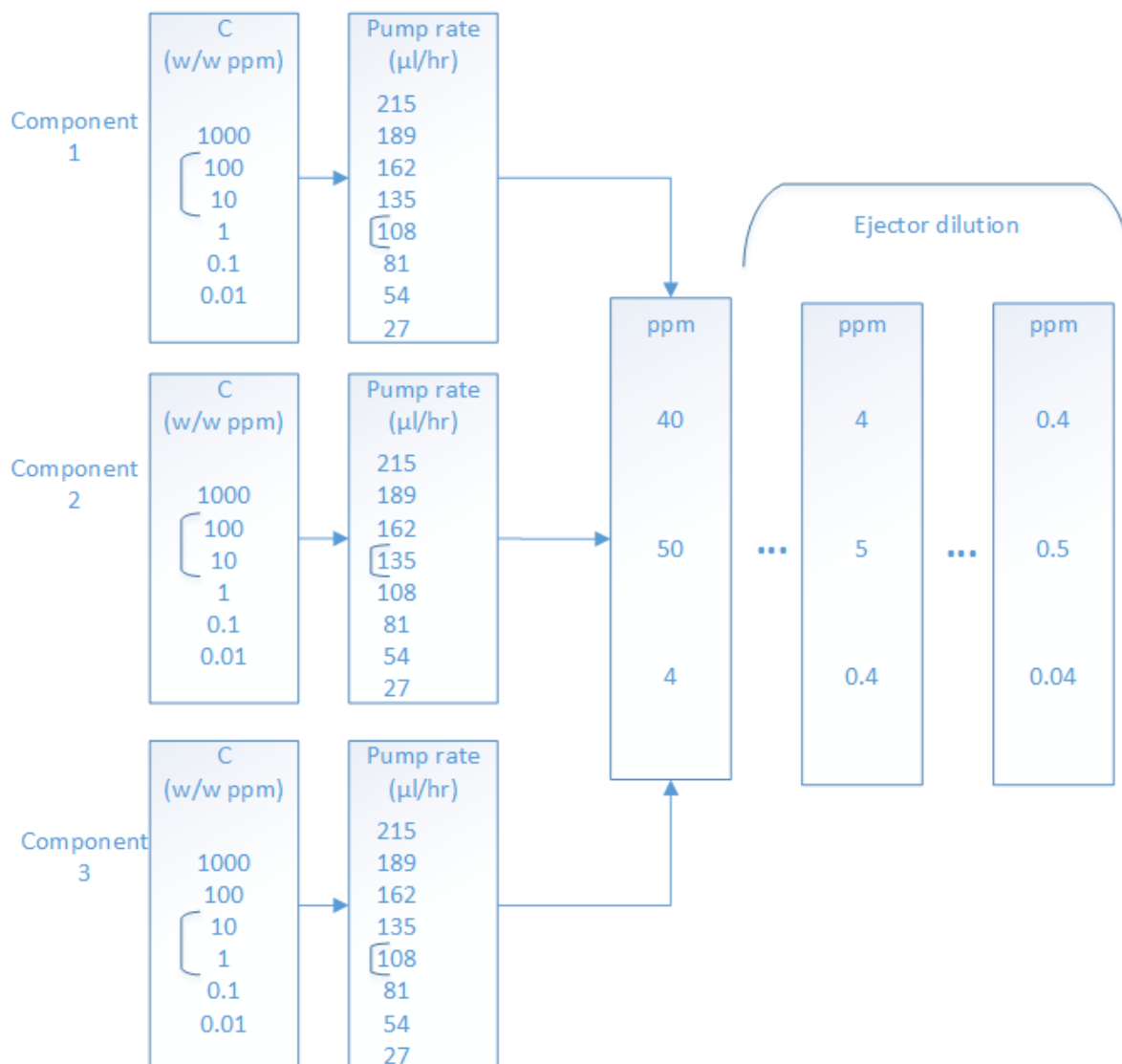


Figure 5. Determination of the produced concentrations. The presented aIMS-O is able to change the concentration of each component with the syringe pumps in a range of one decade. The location of the decade in terms of ppm can be selected with the concentration of the solution used in the syringes. The pump rate of the syringe pumps then determines the gas mass concentration inside that range. Additional ejector dilution stage can be applied to dilute all the components in the same proportion.

dilution, the interrelation of the concentrations between different components remains the same and the whole mixture of components is diluted in same proportion.

Different measurement scenarios were constructed with our olfactometer containing one, two, or three components with the motivation to study and verify how well the compact olfactometer works and how well the different odor components can be distinguished and identified from the ChemPro 100i –data. In one and two component measurements, the remaining empty channels had no odor component and produced, ideally, only clean air.

Figure 6 shows signals from the ChemPro100i –channels detecting negatively charged ions for two different two-component example measurements with BEA and IND with two different concentration pairs. Figure 7 shows the response of single ChemPro 100i-channel in a three-component measurement cycle, where the concentration of CIS is increased gradually.

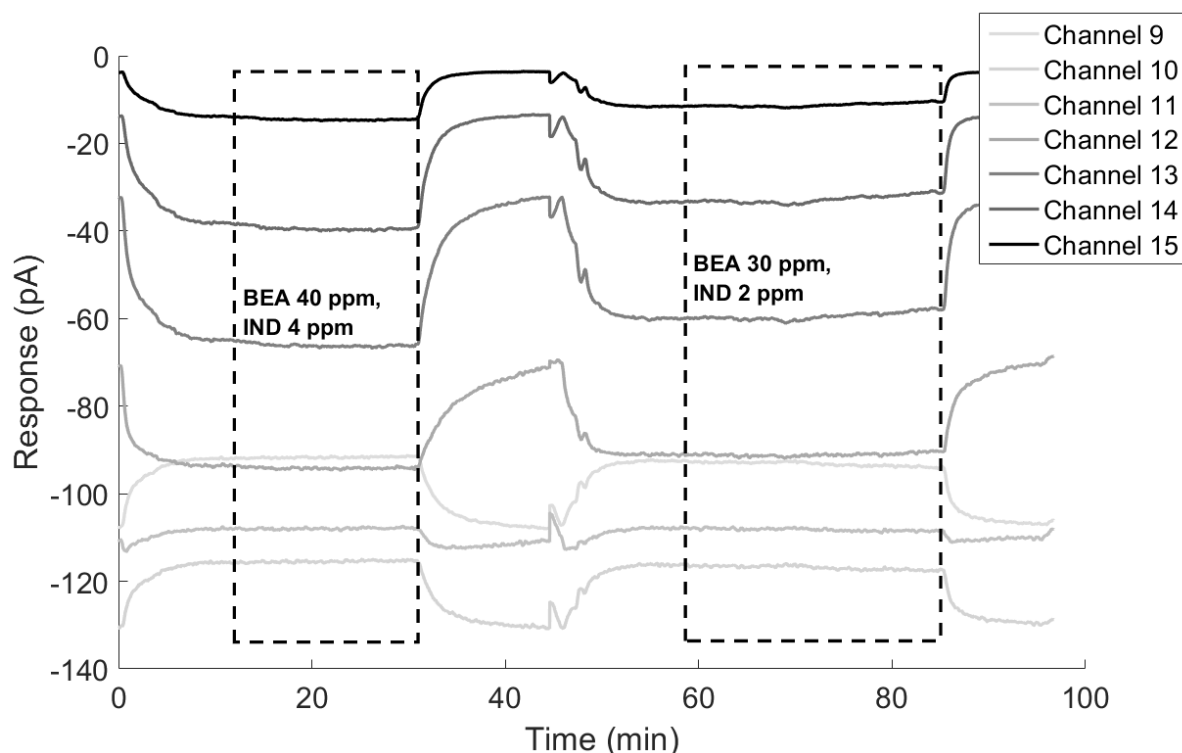


Figure 6. Responses of the negative ChemPro 100i channels over two conducted two component measurements. The stable phases and the estimated gas mass concentrations are marked with dashed lines.

In order to obtain comprehensive information about the odor components or the relationship between different measurements, Sammon mapping is applied in the results section. Sammon mapping is an algorithm for multidimensional scaling, which means that it represents high-dimensional information, the 14 ChemPro-channels in this case, in a space of lower dimensionality (Sammon, 1969). Even though Sammon mapping is considered a non-linear approach, which means that it is difficult to use for actual classification for odors, it still provides useful information and at the very least, tells if signals recorded with ChemPro can be considered identical or if they can be distinguished.

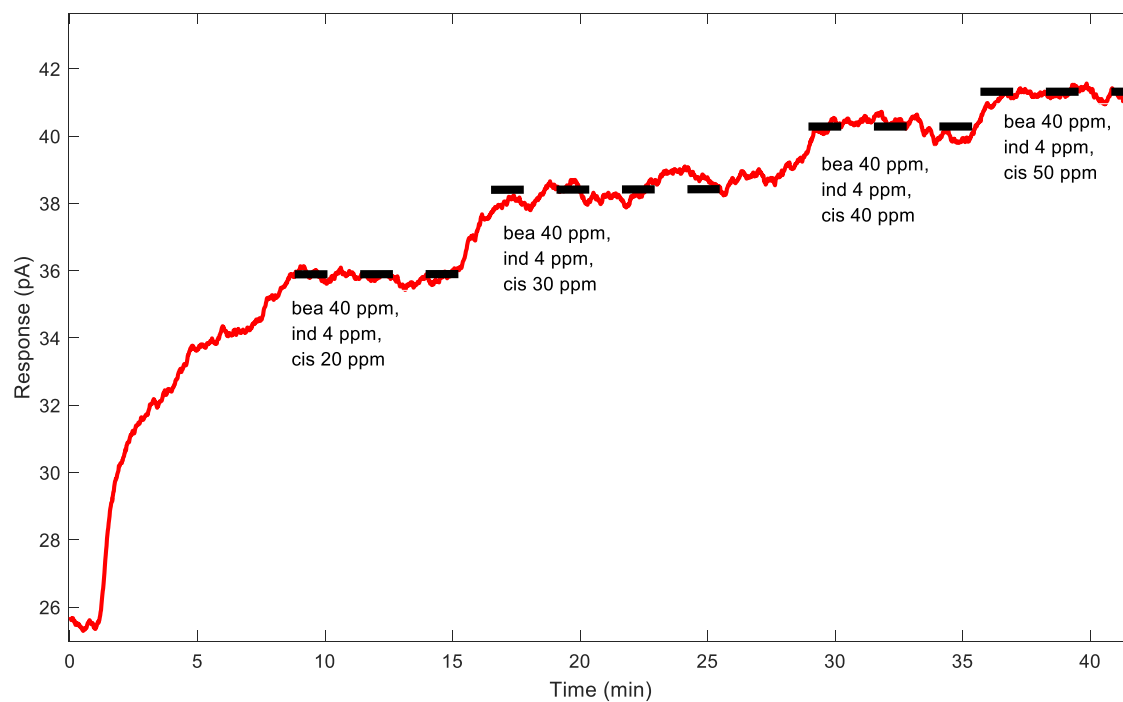


Figure 7. Response from ChemPro 100i channel 6 from a measurement, where the concentration of tertiary synthetic jasmine was increased with gradual increments over a period of 50 minutes. The channel response is relatively stable during the phases emphasized with dotted lines, which implies that the creation of continuous stable concentrations is possible with the olfactometer.

3. RESULTS

In this section, some of the three-component measurement data produced with the aIMS-O is presented using Sammon mapping algorithm. Figure 8 shows Sammon map projection for seven different three-component measurements. Each of the data sets is produced by taking 60 equally spaced data points over a five-minute section from the stable phase of each measurement. Visual inspection of the Sammon map shows that when comparing two datasets with identical concentrations for two of the components, the addition of the third component moves the set in different direction depending which concentration was increased.

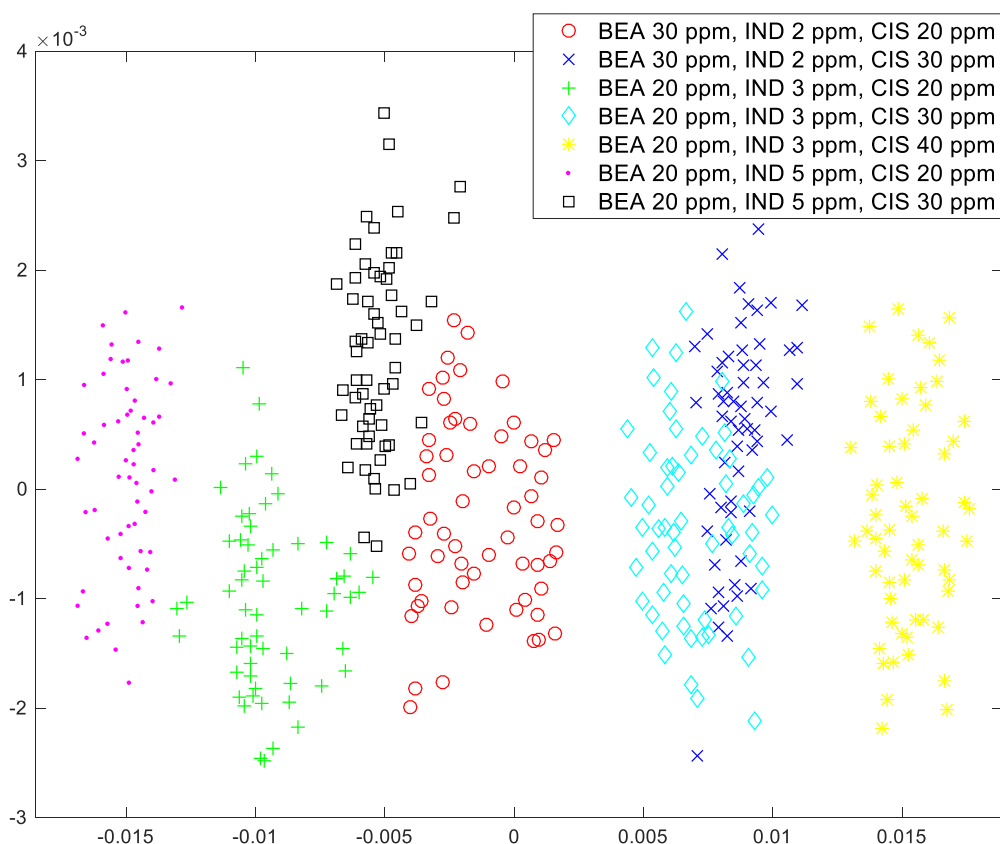


Figure 8. Sammon projection from the Chempro 100i responses for seven concentrations of tertiary synthetic jasmine (IND, CIS, and BEA).

The aIMS-O instrument was also used to conduct measurements with complex solutions in the syringes; diluted jasmine oil and synthetic jasmine oil with two components (BEA and CIS, i.e. binary scent) and three components (BEA, CIS and IND, i.e. tertiary scent). The Sammon map projection of these three stimuli is presented in Figure 9. They were also presented to human participants in pairs to determine if the stimuli were same or different. All the possible combinations of odors were used so that the total of odor pairs presented was nine. The collected data was coded by 1 (same) and 0 (different). A chi-squared test showed a statistical difference from expected frequency when comparing real jasmine oil and binary synthetic jasmine ($\chi^2=6.4$, $p < 0.05$ both when real jasmine was presented first and when binary synthetic jasmine was presented first). These mean differences showed that the two odors were

correctly identified as different. Other tests were not statistically significant, indicating that the participants were not able to judge the rest of the pairs reliably either as same or different. The Sammon map shows similar identification with human perception as the longest distance in the projection is between real jasmine and the binary synthetic jasmine.

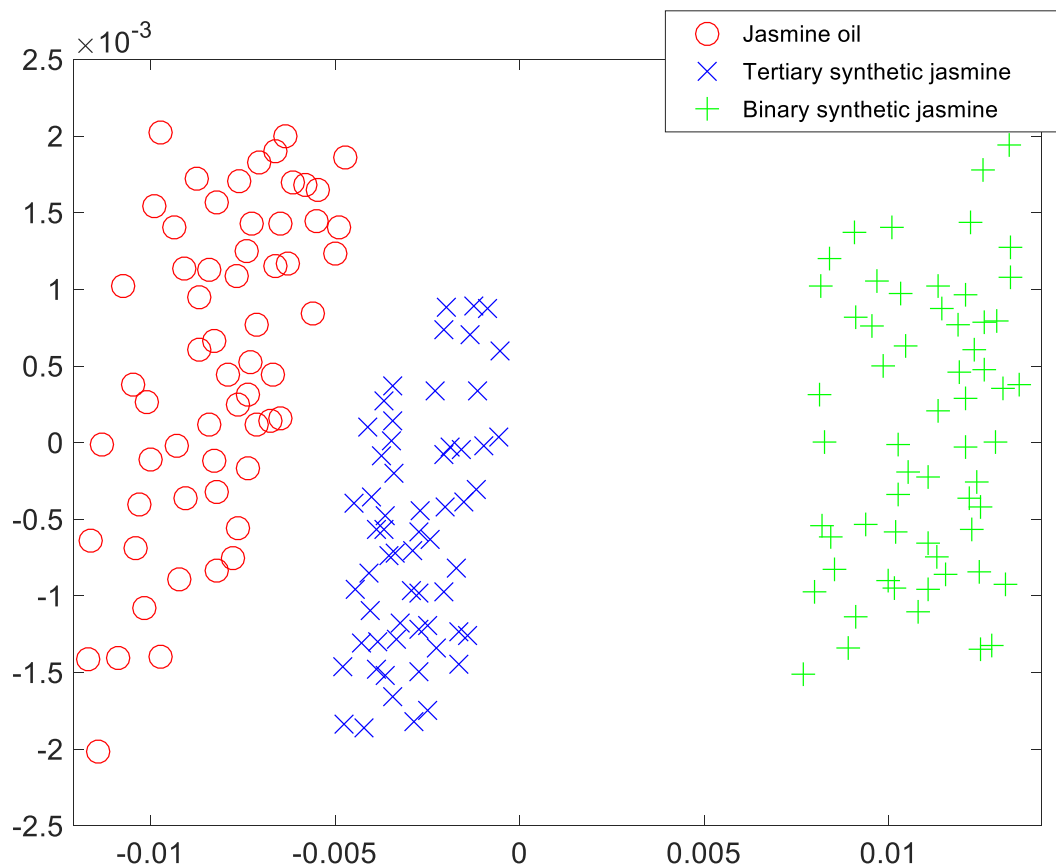


Figure 9. Sammon projection from the ChemPro 100i response for three mixtures: natural jasmine oil, tertiary synthetic jasmine (IND, CIS, and BEA) and binary synthetic jasmine (CIS, BEA).

Human perception between artificial and natural jasmine odors was also tested. Eight participants evaluated whether these two odors were similar. Three different natural jasmine and two different synthetic jasmine concentrations were used. Natural jasmine was evaporated from a bottle headspace and synthetic odor was produced with the olfactometer. Best results occurred with 1 % jasmine and synthetic jasmine containing 70 ppm of BAE, 70 ppm CIS and 7 ppm IND, where only two participants could differentiate the odors. The results are shown in table 1.

Table 1. Human test for differencing synthetic and natural jasmine odor. 1 is for equal perception and 0 for the recognized difference between the odors. Natural jasmine oil was evaporated from a bottle and synthetic odor components with the olfactometer

Natural jasmine oil concentration		0.10 %		1 %		10 %	
concentrations (ppm, w%)	BEA:	40	70	40	70	40	70
	CIS:	40	70	40	70	40	70
	IND:	4	7	4	7	4	7
participant	1	0	0	0	1	0	0
	2	1	1	1	1	1	1
	3	0	1	0	0	0	0
	4	0	1	1	1	0	0
	5	0	0	0	0	0	0
	6	0	0	0	1	0	1
	7	1	1	1	1	1	1
	8	1	1	1	1	1	1
smelled equal		37.5 %	62.5 %	50 %	75 %	37.5 %	50 %
STD		18 %	18 %	19 %	16 %	18 %	19 %

0 different odors, 1 same odors

4. DISCUSSION

The presented aIMS-O instrument is able to produce gas flow with constant, stable gas concentrations of the selected odorants. The relatively long stabilization phase, before the IMS readings become stable, makes it problematic for extensive human testing but based on the ChemPro100i-data measurements with our device are reproducible and useful for further data analysis. With low pumping speeds, the time constants, namely the stabilization phase, became longer as the system first had to fill up the PEEK tube volume of approximately 6 μl before the odor solution reached the heating element. Long waiting times are especially problematic when considering odor perception testing with humans. This problem can possibly be diminished by implementing initial pumping phase to the syringe pump filling up the PEEK tube before actual pumping phase. A more crucial limitation of our instrument is the number of channels being able to handle only three odor components, and even though the external heater tape made the cleansing of the system faster after measurements, total cleansing of the system after long (>60min) measurements proved also to be problematic. The aIMS-O still provides a functional platform for various olfactory-related human perception tests.

There are various limiting factors determining the concentration range able to be produced with our olfactometer. The pumps were driven with 400-step stepper motors and the flow of the odor solution with the lowest possible pumping speeds produced uneven signals. Our tests revealed pumping speeds of 20 $\mu\text{l/hr}$ and lower to be problematic for our olfactometer. One way to mitigate this problem is to change the used syringes to syringes with smaller diameter to achieve larger pumping volume when using the same motor speeds.

The other end of the concentration range is largely determined by the carrying capacity of the carrier gas. If the gas is saturated, increases in pumping speeds do not produce higher concentrations but the odor components start to condense in the tubing walls. This became a problem in our setup when using speeds higher than 220 $\mu\text{l/hr}$. The condensation could be mitigated by heating up the system to a higher temperature, but this would also introduce new problems with the current gas channel adapters containing nitrile, which has heat resistance of 100 °C. Presenting heavily heated gases to human participants would also cause new problems as the temperature of the smelled gas influences perception. Other solution would be increasing the concentration of the odor component in the solution used in the syringes.

The preliminary GC-MS measurements revealed that the system will not cleanse completely after it has been subjected to scent components. Even though the residual scents from previous measurements were only clearly visible in the mass spectrums, they might also distort the IMS-responses. To prevent the interfering effect of possible scent remnants, the airflow from the syringe pump system could be controlled with automated valves.

The results from human perception tests showed that most human participants were unable to distinguish between actual jasmine oil and the synthetic tertiary jasmine. This is in line with findings that only a few components can be used to successfully mimic the organoleptic properties of an authentic odor if the properties of ratios are matching, and the components are so called key odor components (i.e., odorous molecules that carry most of the organoleptic properties of an odor). The device has also successfully been used in a number of other human tests, including integrated with virtual reality (VR).

Human perception tests revealed noticeable similarity with the synthetic jasmine and the jasmine oil. With three component synthetic jasmine and jasmine oil 37.5–70 percent of the participants evaluated the odors to be equal. According the ion mobility data in Figure 10, the three-component synthetic jasmine is closer to jasmine oil odor than

two component odor. This is in line with human perception tests, but as human perception is rather subjective and varies from person to person so in terms of objectivity, ChemPro 100i performs notably better. It remains to be studied more carefully how similarly IMS and human perception mechanisms work. Here we had only a snapshot what revealed some similarities when few components are mixed.

References

- Auffarth, B. (2013) ‘Understanding smell — The olfactory stimulus problem’, *Neuroscience and Biobehavioral Reviews*. Elsevier Ltd, 37(8), pp. 1667–1679. doi: 10.1016/j.neubiorev.2013.06.009.
- Benedetti, S. *et al.* (2005) ‘Shelf Life of Crescenza Cheese as Measured by Electronic Nose’, *Journal of Dairy Science*, 88(9), pp. 3044–3051. doi: 10.3168/jds.S0022-0302(05)72985-4.
- Bensafi, M. *et al.* (2003) ‘Perceptual, affective, and cognitive judgments of odors: Pleasantness and handedness effects’, *Brain and Cognition*, 51(3), pp. 270–275. doi: 10.1016/S0278-2626(03)00019-8.
- Berna, A. (2010) ‘Metal oxide sensors for electronic noses and their application to food analysis’, *Sensors*, 10(4), pp. 3882–3910. doi: 10.3390/s100403882.
- Brooks, S. W. *et al.* (2015) ‘Canine Olfaction and Electronic Nose Detection of Volatile Organic Compounds in the Detection of Cancer: A Review ’, *CANCER INVESTIGATION*. PHILADELPHIA : TAYLOR & FRANCIS INC , pp. 411–419. doi: 10.3109/07357907.2015.1047510.
- Chu, S. and Downes, J. J. (2000) ‘Odour-evoked autobiographical memories: psychological investigations of proustian phenomena.’, *Chemical senses*. England, 25(1), pp. 111–116.
- Doty, R. L., Reyes, P. F. and Gregor, T. (1987) ‘Presence of both odor identification and detection deficits in Alzheimer’s disease.’, *Brain research bulletin*. United States, 18(5), pp. 597–600.
- Eiceman, G. A., Karpas, Z. and Hill, H. H. (2013) *Ion mobility spectrometry*. 3rd edn. CRC Press.
- Fang, X. F. X. *et al.* (2010) ‘Determination of Ammonia Nitrogen in Wastewater Using Electronic Nose’, *Bioinformatics and Biomedical Engineering (iCBBE), 2010 4th International Conference on*, pp. 1–4. doi: 10.1109/ICBBE.2010.5515426.
- Friedrich, M. J. (2009) ‘Scientists seek to sniff out diseases electronic “noses” may someday be diagnostic tools ’, *JAMA - Journal of the American Medical Association* . CHICAGO : AMER MEDICAL ASSOC , pp. 585–586. doi: 10.1001/jama.2009.90.

Giordani, D. S. *et al.* (2007) 'Biodiesel characterization using electronic nose and artificial neural network', (September), pp. 16–20.

Glatz, R. and Bailey-Hill, K. (2011) 'Mimicking nature's noses: From receptor deorphaning to olfactory biosensing', *Progress in Neurobiology*. Elsevier Ltd, 93(2), pp. 270–296. doi: 10.1016/j.pneurobio.2010.11.004.

Guichard, E. (2017) *Flavour: from food to perception*. Chichester, West Sussex Hoboken, NJ: John Wiley & Sons Inc.

Gutiérrez, J. and Horrillo, M. C. (2014) 'Advances in artificial olfaction: Sensors and applications', *Talanta*, 124, pp. 95–105. doi: 10.1016/j.talanta.2014.02.016.

Hedner, M. *et al.* (2010) 'Cognitive factors in odor detection, odor discrimination, and odor identification tasks.', *Journal of clinical and experimental neuropsychology*. England, 32(10), pp. 1062–1067. doi: 10.1080/13803391003683070.

Huotari, M. (2004) *Odour Sensing by Insect Olfactory receptor neurons: Measurements of Odours based on Action Potential analysis*.

James, D. *et al.* (2005) 'Chemical sensors for electronic nose systems', *Microchimica Acta*, 149(1–2), pp. 1–17. doi: 10.1007/s00604-004-0291-6.

Kolakowski, B. M. *et al.* (2007) 'Analysis of chemical warfare agents in food products by atmospheric pressure ionization-high field asymmetric waveform ion mobility spectrometry-mass spectrometry', *Analytical Chemistry*, 79(21), pp. 8257–8265. doi: 10.1021/ac070816j.

Labreche, S. *et al.* (2005) 'Shelf life determination by electronic nose: Application to milk', *Sensors and Actuators, B: Chemical*, 106(1 SPEC. ISS.), pp. 199–206. doi: 10.1016/j.snb.2004.06.027.

Laing, D. G. and Glemarec, A. (1992) 'Selective attention and the perceptual analysis of odor mixtures', *Physiology and Behavior*, 52(6), pp. 1047–1053. doi: 10.1016/0031-9384(92)90458-E.

Lamagna, A. *et al.* (2008) 'The use of an electronic nose to characterize emissions from a highly polluted river', *Sensors and Actuators, B: Chemical*, 131(1), pp. 121–124. doi: 10.1016/j.snb.2007.12.026.

Livermore, A. and Laing, D. G. (1998) 'The influence of chemical complexity on the perception of multicomponent odor mixtures', *Perception & Psychophysics*,

60(4), pp. 650–661. doi: 10.3758/BF03206052.

Lundström, J. N. *et al.* (2010) ‘Methods for building an inexpensive computer-controlled olfactometer for temporally-precise experiments’, *International Journal of Psychophysiology*, 78(2), pp. 179–189. doi: 10.1016/j.ijpsycho.2010.07.007.

Nakamoto, T., Kakizaki, M. and Suzuki, Y. (2004) ‘Response analysis of odor sensor based upon insect olfactory receptors using image processing method’.

Omatu, S. (2013) ‘Odor classification by neural networks’, *Proceedings of the 2013 IEEE 7th International Conference on Intelligent Data Acquisition and Advanced Computing Systems, IDAACS 2013*, 1(September), pp. 309–314. doi: 10.1109/IDAACS.2013.6662695.

Phillips, M. *et al.* (2003) ‘Detection of lung cancer with volatile markers in the breath.’, *Chest*. United States, 123(6), pp. 2115–2123.

Richardson, B. E. *et al.* (2004) ‘Altered olfactory acuity in the morbidly obese.’, *Obesity surgery*. United States, 14(7), pp. 967–969. doi: 10.1381/0960892041719617.

Sammon, J. W. (1969) ‘Nonlinear Mapping Structure Analysis’, *IEEE Transactions on Computers*. C-18 (5), pp. 401-409.

Schaller, E., Bosset, J. O. and Escher, F. (1998) “‘Electronic Noses’ and Their Application to Food’, *Lebensmittel-Wissenschaft und-Technologie*, 31(4), pp. 305–316. doi: 10.1006/fstl.1998.0376.

Schmidt, R. and Cain, W. S. (2010) ‘Making scents: dynamic olfactometry for threshold measurement.’, *Chemical senses*. Oxford University Press, 35(2), pp. 109–20. doi: 10.1093/chemse/bjp088.

Sommer, J. U. *et al.* (2012) ‘A mobile olfactometer for fMRI-studies’, *Journal of Neuroscience Methods*. Elsevier B.V., 209(1), pp. 189–194. doi: 10.1016/j.jneumeth.2012.05.026.

Spence, C. (2010) ‘The multisensory perception of flavour’, *Psychologist*, 23(9), pp. 720–723. doi: 10.1016/j.concog.2007.06.005.

Stevenson, R. J. (2010) ‘An initial evaluation of the functions of human olfaction.’, *Chemical senses*. England, 35(1), pp. 3–20. doi: 10.1093/chemse/bjp083.

Tang, K.-T. *et al.* (2010) ‘Development of a Portable Electronic Nose System for

the Detection and Classification of Fruity Odors’, *Sensors*. doi: 10.3390/s101009179.

Thomas-Danguin, T. *et al.* (2014) ‘The perception of odor objects in everyday life: a review on the processing of odor mixtures’, *Frontiers in Psychology*, 5(June), pp. 1–18. doi: 10.3389/fpsyg.2014.00504.

Utriainen, M., Kärpänoja, E. and Paakkanen, H. (2003) ‘Combining miniaturized ion mobility spectrometer and metal oxide gas sensor for the fast detection of toxic chemical vapors’, *Sensors and Actuators, B: Chemical*, 93(1–3), pp. 17–24. doi: 10.1016/S0925-4005(03)00337-X.

Wilson, A. D. and Baietto, M. (2009) ‘Applications and Advances in Electronic-Nose Technologies’, *Sensors*, 9(1), pp. 5099–5148. doi: 10.3390/s110101105.